Mechanical Properties of 304-Steel Springs in Cryogenic Environment

Ian Rhudy*
University of Michigan, Department of Physics
Virginia Tech, Department of Physics
(NSF REU)

Nathan Dressler†
Virginia Tech, Department of Physics
(Dated: July 22, 2024)

The DarkSide-20k liquid Argon time-projection chamber (TPC) is planned to use 2472 spring-tempered 304 stainless steel springs in the support of a 1236 wire grid. Liquid argon has a boiling point of 87 K, exposure to which causes the Young's Modulus of 304 stainless to increase, influencing the spring constant (k) and pretension (T_p) of the springs. Compared to the ambient temperature value of k= 78.19 ± 0.12 N/m, k was measured to increase to 82.45 ± 0.12 N/m (5.5 ± 0.2 %) using liquid nitrogen (LN2) and its boil off to reach temperatures at 87 K. The pretension was also qualitatively measured to stay roughly constant at 1.46 N, while the length of the spring was qualitatively measured to decrease by about 400 microns. The experimental apparatus consisted of a 0.848 in clear T-shaped PVC in which the spring was housed, allowing chilled N2 gas/liquid to be blown normally to the direction of oscillation. Using a temperature probe in this encasing, oscillations were videoed over a range of temperatures with which the spring constant could be determined. Measurement of these parameters minimizes the uncertainty involved in building such a nuanced and complicated detector.

I. INTRODUCTION

A. DarkSide-20k

As a time projection chamber, DarkSide-20k is built to determine the precise 3D location and energy of high-energy particle events via scintillation. The name "time-projection chamber" hints at how DS-20k will accomplish this: by comparing the detection times of two different scintillation signals (S1 and S2), we will be able to determine the energy and 3D location of high energy particle events in the detector. S1 is generated by the scintillation of liquid argon (LAr) filling the detector and is measured via a plane of photo-multiplier tubes at the top and bottom of the detector. The event producing this scintillation light also frees electrons in the LAr, and, with the help of a -73.38 kV cathode at the bottom of the detector, will cause electrons to drift up through the detector at a well-defined speed.

At the top of the detector will be a wire grid at approx. -4kV (suspended by the springs addressed by this paper), followed 1cm later by an anode. Once the electrons reach this wire grid, the gradient of the voltage increases from 200 V/cm to 4.2 kV/cm, accelerating electrons to the point of electro-luminescence. The time difference between the reception of the electro-luminesced S2 signal and the S1 can then be used to determine the z height of the event, as the electrons move at a predictable velocity down the potential gradient. A diagram of the DarkSide-20k TPC is shown in FIG. 1:

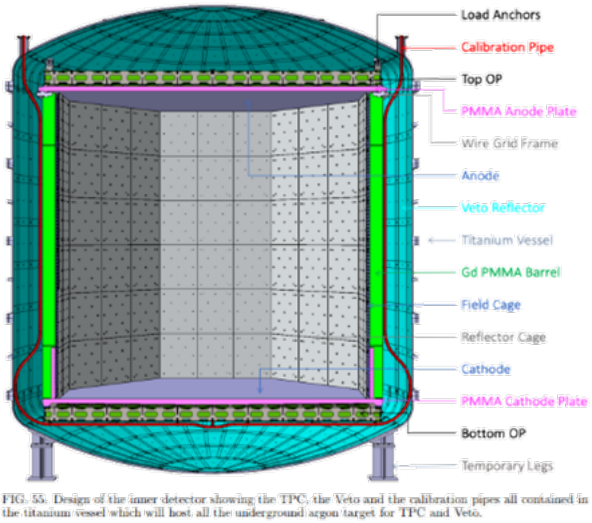

FIG. 55. Design of the inner detector showing the TPC, the Veto and the calibration pipes all contained in the titanium vessel which will host all the underground argon target for TPC and Veto.

FIG. 1. DarkSide-20K Detector; Notice the mirror-plated cavity for liquid Argon, Cathode, Anode, and Wire Grid

The necessity of a spring-supported wire grid lies in the behavior of the detector while LAr is in the process of reaching thermal equilibrium. As will be addressed later, all materials experience a change in physical properties with a change in temperature, including contraction and stiffening when cooled. At 87 K, the wire frame will experience relatively large amounts of contraction when cooling from ambient to equilibrium with the LAr, but

* ianrhudy@umich.edu
† nathand04@vt.edu

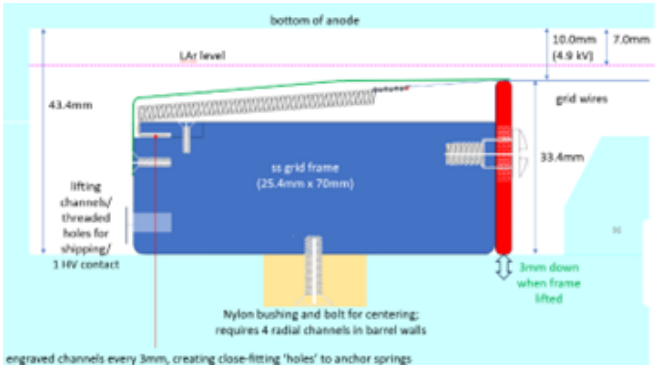

FIG. 2. Spring suspension design in DS20k; In red is the bridge plate, green is the Faraday Cage, and grid frame in blue. Notice the potential for frictional effects due to the wire's angle of attack with the bridge plate.

this cooling process will be nonuniform. The center of the wire grid will cool before the perimeter, which, without springs, would increase the strain on the wires and potentially cause breakage. The springs allow any nonuniform changes in tension to be compensated for via elongation of the springs, keeping the stresses off the wires themselves. The implementation of these springs is depicted in FIG. 2.

B. The Spring and Young's Modulus

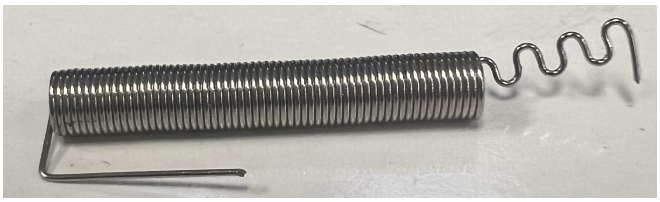

FIG. 3. Spring-tempered 304 Stainless Steel Spring used in DS-20k; notice the 66 coils, square hook, and switchback hook coils for wire attachment.

The spring design (FIG. 3) itself is also equipped with a number of "neat features" that keep the wire grid as stable as possible. With a spring-tempered wire diameter of 300 micrometers, inner spring diameter of 2.5 millimeters, room temperature Young's Modulus of 200 GPa, and Poisson ratio of 0.275, we can predict the spring constant to be in the range of 70 - 80 N/m using the following equation:

$$k = \frac{Ed^4}{16(1+\nu)nD^3} \tag{1}$$

Where d is the wire diameter, D is the spring's inner diameter, E is Young's Modulus, ν is the Poisson ratio, and n is the number of coils (66). Notice the 4th and 3rd power dependence of d and D respectively, meaning that any small error in our measurement of these values will result in a much larger variation in k. As such, this formula is useful only as a general approximation, or to compare the percent change in k with temperature (as will be expanded on later).

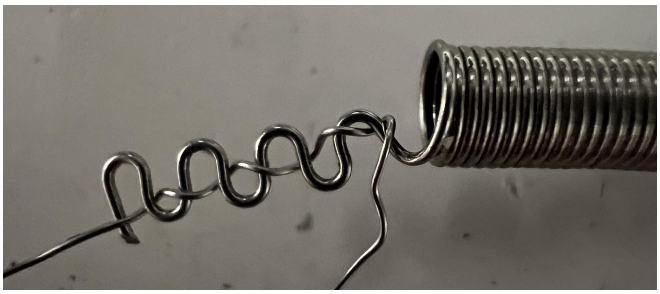

FIG. 4. Attachment of the wire to the spring via switchback hook; The interlacing of the wire with the spring causes enough friction to keep the wires from detaching at up to 10N

The method of connecting the springs to the wire grid features the use of a switchback hook, shown in FIG. 4. By bending the trailing wire back and forth on itself in a repeating "S" pattern, the wires making up the grid can be woven into the tail of the spring, making it so that a large force on the wire only strengthens the connection to the spring (up to about 10 N - the point where the switchback hook bends). As you tug on the wire, it attempts to slide past the coils of the switchback hook, but the bend in the wire causes a large component of the "tug" force to push the wire into the switchback hook, thereby increasing friction dramatically. The fact that this process occurs for all 4 loops of the switchback hook means that the net force opposing the tug is large enough to prevent slippage.

The most important concept for this experiment, however, is the temperature dependence of Young's Modulus. Young's Modulus (E) is defined as the ratio of a materials stress (force/area) per strain ($\Delta L/L$), thereby quantifying the amount of stress needed to deform a material by a certain amount. Conceptually, this is a measure of the "stiffness" of a material.

The most important aspect of E for this experiment is the fact that it is inversely proportional to temperature (T) - as T increases, E increases. The relationship between 304 stainless' E with temperature is depicted below in FIG. 5. This increase in E with a decrease in T can be explained by considering the motions of the atoms in a warm vs. cold material, and the fact that the inter-atomic forces obey the Lennard-Jones potential (the closer two atoms are, the stronger the attraction up until a certain minimum where the force becomes repulsive).

In a warm material, as compared to a cold one, the atoms are jiggling around with lots of kinetic energy, meaning on average they sit farther up the potential well, and are thus farther apart, than if they were stationary. Atoms that are farther apart have a weaker force of at-

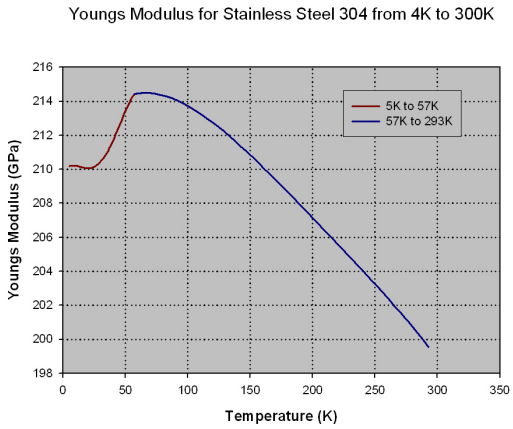

FIG. 5. E vs. Temperature for 304 Stainless [1]. Only temperatures as low as 83K are measured in this experiment, and the plot above considered non-spring-tempered wire while ours is. Note: this plot only gives us a general trend and scale of the behaviour of our spring with temperature - specific calculated values will not necessarily match due to the nuanced differences between our wire and that depicted above.

traction (with the attractive part of the Lennard-Jones potential going as $1/r^6$), which, when summed over millions and millions of atoms, contributes to a noticeable decrease in the "stiffness" of a warm material compared to a cold one. Essentially, the atoms of a cold material are more "locked in place" than the atoms of a warm material, simply because the atoms of a warm material are bouncing and moving around much more than a cold material. As I mentioned above, we defined E to be a measure of such "stiffness," meaning it is affected by temperature.

In preparation for our k vs. T measurements, we can predict what sort of general trend to expect using EQU. 1 in conjunction with FIG. 5 and the specifications of the wire. Note: This prediction can only give a general scale for our δk expectation, as there are a number of minute differences between EQU. 1 in theory and our actual spring in practice. For examples, our wire is spring-tempered, pretensioned, and features a square hook at the end, all of which cause deviations (albeit small) with the result predicted by EQU. 1. Using EQU. 3 with E = 214.5 GPa at 87K and 199.5 GPa at 290K, we can calculate (k = 83.6 N/m) and (k = 78.0 N/m) respectively, corresponding to a:

$$\frac{83.6 - 78.0}{78.0} = 6.8\% \tag{2}$$

increase in k at 87K compared with 290K.

The pretension and length of the spring also change as a function of temperature, though these parameters are not nearly as important for the DS20K experiment as k is (nor are they as obvious to measure). The change in length of a material with temperature is given by:

$$\Delta L = \alpha * \Delta T * L \tag{3}$$

where alpha is the coefficient of thermal expansion unique to each material and ΔT is the change in temperature. In our case, $\alpha = 1.73 * 10^{-}5\frac{m}{m*K}$ for 304 stainless. ΔL in our experiment can be shown to be extremely small, as, taking an extreme example that we have a length of wire 17 inches (.43m) long instead of a spring exposed to 87 K, the contraction from 290K would be:

$$\Delta L = \alpha * \Delta T * L = \mathbf{1.5mm} \tag{4}$$

So, even a wire 17 in long would have near negligible ΔL over the temperature range in our experiment, meaning the change in length of our spring will be even harder to detect. As such, only the general trend of length contraction will be observed.

The pretension is similarly difficult to measure; in addition to only very small changes taking place over our temperature range, the actual mechanics of pretensioning springs is a complicated process. As little as 1 missed twist in the spring's construction can influence the pretension distribution across the spring, so there is no way to reliably predict how to a certain pretension changes with temperature. (Nonuniform pretension causes a nonuniform stretch of the spring as temperature changes, impairing our ability to measure the stretch of the spring as a pretension diagnostic; See FIG. 6). As such, we can only comment on the general trend we see the pretension follows with temperature.

FIG. 6. A demonstration of nonuniform pretension in a spring; a specifically chosen mass is hung from the spring such that it has enough weight to overcome the pretension of the lower half of the spring but not the upper half - as seen in the prevalence of gaps between coils in the lower but not upper half.

Measurements of these properties of the spring are important in the context of DS-20k due to the harsh conditions the springs will be exposed to. The frame of the detector will increase in stiffness with the cold in addition to the change in k. If the change in k were to be much greater than a linear dependence with E, the springs would pull more than they did at ambient temperatures with respect to the frame, potentially causing deformations. Similar disproportionate increases in k could exceed the elastic limit of the wires or the holding capacity of the switchback hook, both of which would be catastrophic to the multi-million dollar detector. It is the goal of this experiment to quantify any changes in k to ensure the 304 steel springs will behave appropriately in the cryogenic detector.

II. MATERIALS AND METHODS

A. Design of Cryogenic Housing

At 206K below ambient, keeping springs consistently at 87K requires the design of appropriate housing. Final experimental designs include a Nitrogenous glove-box, humidity sensor, PVC T-Connector blowing LN2, and a T-Type thermocouple, all surrounding the spring hanging from a 14" lab stand.

A Nitrogenous atmosphere is necessary for the mitigation of water vapor condensation on the spring (frosting). Such condensation would tamper with the springs stretch-compression rate, thereby influencing the spring constant (k). Such a Nitrogenous atmosphere is realized via glove-box housing the spring oscillation apparatus (FIG. 7). Two holes were cut into the side of a 95 Qt. clear plastic tote through which rubber gloves could be inserted and clamped, allowing interaction with the spring without water vapor contamination. A consistent N2 atmosphere was realized by "purging" the box with N2 ambient air before experiments took place. The progress of the purge was measured by a SHT45 humidity probe connected to an Arduino LCD. Once the relative humidity reached below 14% the N2 air flow was stopped and LN2 could successfully flow into the box without risk of frosting.

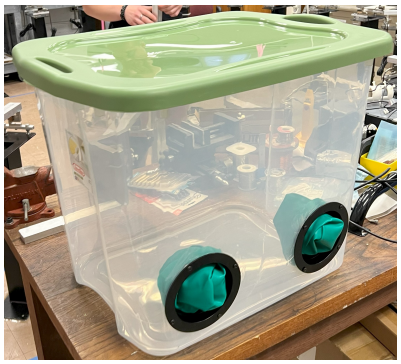

FIG. 7. Myco Labs Glove-box designed to mitigate frosting

Aside from frosting, it is also of vital importance to ensure maximum concentrated cooling of the spring. Previous version of the experiment demonstrated that N2 evaporation warmed too quickly in just a few centimeters above the LN2 level, reaching 140K at 5 cm above the surface. It thus became apparent that a direct, concentrated stream of N2 blow off was needed relatively directly from liquid N2. This was obtained by utilizing a PVC T-Connector oriented such that N2 blow-off would flow normally to the spring's axis of oscillation, allowing only a small volume to be cooled around the spring while minimizing drag. The size of volume is very important in determining cooling efficiency, as the larger the volume the more mass must be cooled in order to reach equilibrium with the N2 coolant. LN2 was to flow down the hose before evaporating upon contact with the PVC, placing the spring within 1 cm of the LN2 source. The amount of LN2 flowing into the PVC and thus evaporating to cool the spring could be changed to control temperature, allowing for as low as 84K to be maintained consistently within 1K. See FIG. 8 for the PVC housing setup.

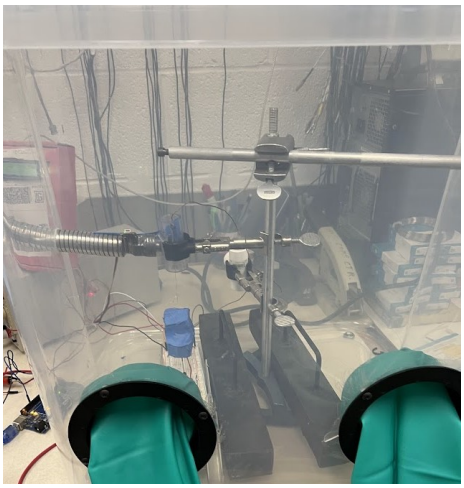

FIG. 8. PVC spring housing concentrates the N2 blow-off

Inside the PVC house is a T-Type Thermocouple to measure the temperature of the spring. Rated for temperatures from 3K to 640K, the thermocouple could withstand even direct contact with LN2, measuring temperature to an accuracy of ±1K. In this way oscillations could be recorded at various temperatures to determine k's behaviour with T.

B. Spring Constant, Length, and Pretension Measurements

1. *Spring Constant*

The determination of the spring constant relies only on its simple harmonic motion. It was determined qualitatively that only negligible dampening was present in the spring oscillations, thereby allowing k to be determined directly by the relation:

$$k = m * (\frac{n * 2\pi}{t_n})^2 \tag{5}$$

where m is the mass of a weight hanging from the spring, n is a certain number of oscillations, and t_p is the time it takes for n oscillations. In this way, the measurement of the period for 60 oscillations at various temperatures will allow calculation for k.

To determine this period, a video is taken of the spring oscillation at each temperature. Then, video analysis software can be used to step frame by frame through the oscillation to record the precise moment when 60 oscillations end. However, the duration of a frame at 60 fps

is 0.016 s, meaning the "precise" end of an oscillation can only be determined within 0.016 s of the actual end. This error can be reduced, however, by timing the oscillation for a large number of cycles; the error in frame length for 60 oscillations is only 0.12 N/m, so we set n = 60 in the above equation. See FIG. 9 for a view of the frame-stepping software.

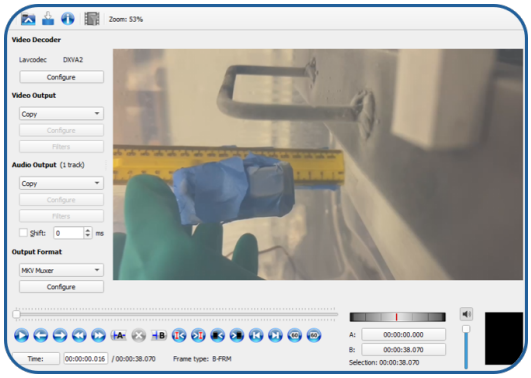

FIG. 9. Avidemux Video Analyzer was used to determine the start and end frames of an oscillation.

Recording the temperature in the audio of each oscillation video recording allows for the appropriate k value to be tabulated with its appropriate T value.

2. *Length Contraction*

By hanging a weight of 1N on the spring, the magnitude of length contraction can be measured without the influence of a changing k or T_p. 1N is not enough to overcome the inbuilt pretension of the spring, thus any change in height of weight as the spring is cooled is only due to the contraction of the spring itself. This change in height due to length contraction alone (ΔL) can then be measured by placing a camera in the glove box system, recording the height with a ruler at various temperatures. However, as demonstrated in the introduction, the (ΔL) will be very small for our length of spring, on the order of microns. As such, we can only determine a change in height from the warmest to the coldest temperature, interpolating with a linear function in between. Such an approximation can be made due to the small (ΔL), as any function becomes linear when changes are small enough. See FIG. 10 for a diagram of this setup.

3. *Pre-tension Measurement*

Pretension can be determined in a similar manner to length contraction, replacing a 1N weight with a 3N weight. The 1N weight was used to keep the spring coiled, measuring how the cold changed the actual length of the spring. However, a 3N mass stretches the spring, allowing the effects of Δk and ΔT_p to be determined. The

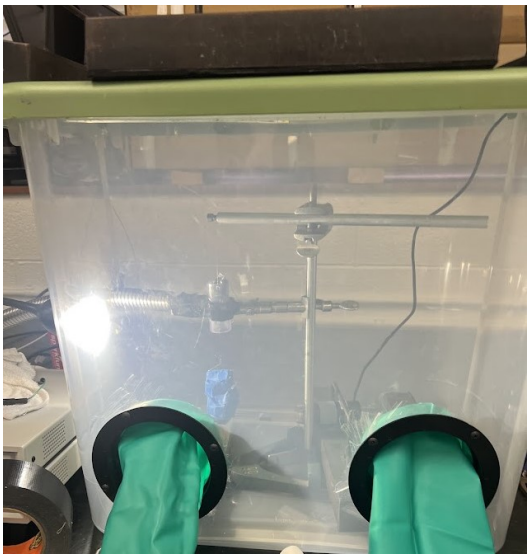

FIG. 10. Camera-integrated glove-box for length contraction measurements

equation relating pretension, length contraction, and the spring constant are given in FIG. 11 below:

$$T_p(T) = mg - k(T)[\Delta S + \Delta L(T) - \Delta h(T)] \quad (6)$$

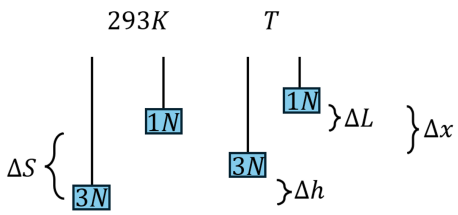

FIG. 11. Depiction of changing length values with temperature

Where mg = 3N, k(T) is the measured spring constant at a certain temperature, ΔS is the length of the spring at ambient temperature with a 3N weight, ΔL is the measured contraction of the spring at a certain temperature, and Δh is the measured change in height of the spring with a 3N mass at a certain temperature. Plugging in these known values into the equation can give the change in pretension of the spring due to temperature, but, as mentioned in an earlier section, difficulties arise due to nonuniformities in the pretension and the scale of the changes involved. A depiction of the pretension measurement is shown below in FIG. 12. Because it is calculated from other independent variables, the error in pretension is given by the multi-variable calculus formula, where δ signifies the error in the measured value:

$$\delta T_p = ((\frac{\partial T_p}{\partial \Delta h} * \delta\Delta)^2 + (\frac{\partial T_p}{\partial k} * \delta k)^2 + (\frac{\partial T_p}{\partial \Delta L} * \delta\Delta L)^2 + (\frac{\partial T_p}{\partial \Delta S} * \delta\Delta S)^2)^{\frac{1}{2}} \quad (7)$$

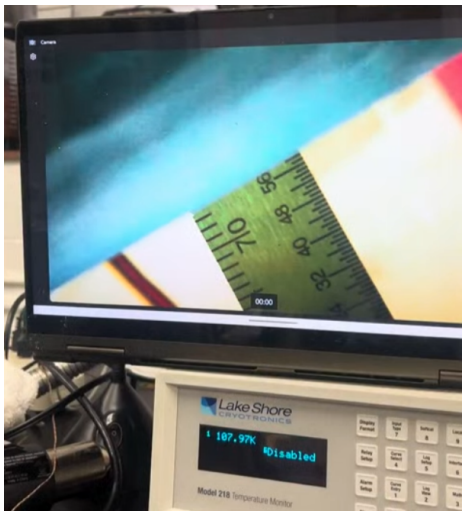

FIG. 12. Screenshot of a measurement of Δh used in the pretension calculation

III. RESULTS

Using the experimental outline from above, k was measured at temperatures ranging from 290K to 83K, depicted in FIG. 13. An increase of 5.5% was measured in k between 290K and 87K, ±0.2%. A fourth-degree polynomial fit was determined for this data:

$$k(T) = (9.68 * 10^{-10})T^4 - (6.98 * 10^{-7})T^3 + (1.52 * 10^{-4})T^2 - (3.16 * 10^{-2})T + 84.49 \quad (8)$$

Rudimentary error bars were also calculated by assuming most error was due to the resolution of period length due to frame rate, producing an error of about ± 0.12 N/m per k. Horizontal error bars were also determined by assuming the maximum variation in temperature measured occurred for each k measurement, producing horizontal error bars of roughly 1K.

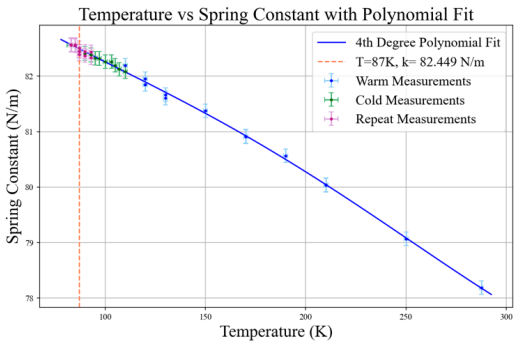

FIG. 13. Measured values of k vs. temperature over a cryogenic range. Purple points represent repeated trials to ensure consistent measurements.

The length of the un-stretched spring (FIG. 14) and the length of the stretched spring (FIG. 15) were then measured at 290K and 77K, creating linear fits of $\Delta L = -0.0019T + 0.5525$ and $\Delta h = -0.0072T + 2.0619$. Errors in this measurement were due to the mass slightly oscillating, but these error could be made as small as 0.1mm with only slight deviations.

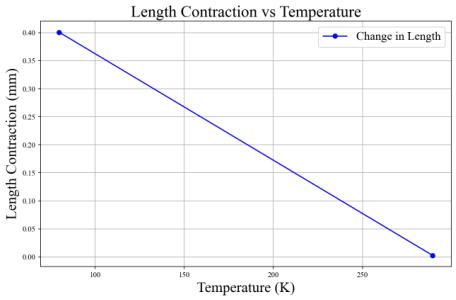

FIG. 14. Measurement of ΔL at 77K and 290K allowed for a linear fit to be interpolated for pretension calculations.

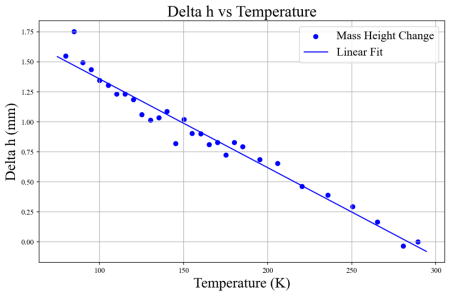

FIG. 15. The height of a 3N mass on a spring vs. temperature, including a linear fit.

Finally, ΔS was measured to be 0.019 m, allowing for the above values to be plugged into EQU. 6 to determine the value of T_p with temperature (FIG. 16), who's error is based solely on the error of the preceding measurements. Tabulated data is shown below.

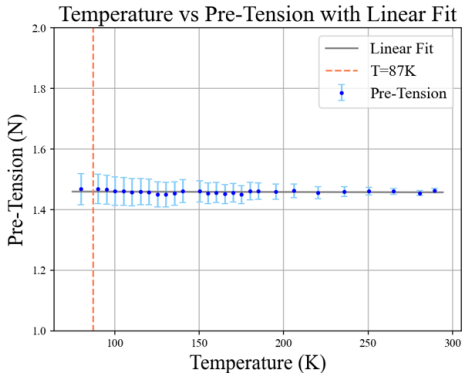

FIG. 16. Plot of T_p with temperature. Notice error at colder temperatures prevents concluding the specific slope of the trend, but regardless pretension stays roughly constant.

T(K)	k(N/m)	T(K)	k(N/m)
83	82.562	107	82.125
85	82.558	110	82.082
87	82.449	120	81.851
90	82.408	130	81.667
93	82.257	149	81.667
95	82.321	170	80.915
97	82.318	190	80.567
100	82.261	210	80.036
103	82.261	250	79.070
105	82.196	288	78.187

T(K)	Δh(mm)	T_p(N)	T(K)	Δh(mm)	T_p(N)
79.85	1.55	1.47	155.03	0.9	1.45
84.85	1.75	1.49	160.09	0.9	1.46
89.96	1.49	1.47	165.09	0.81	1.45
94.92	1.44	1.47	170.05	0.83	1.46
100	1.35	1.46	175	0.72	1.45
105.16	1.31	1.46	180.03	0.83	1.46
110.09	1.23	1.46	184.97	0.79	1.46
125.14	1.06	1.45	220.33	0.46	1.46
135.18	1.03	1.45	250.51	0.29	1.46
145.12	0.82	1.44	280.58	-0.03	1.45
150.09	1.02	1.46	289.34	0	1.46

IV. CONCLUSION

The main takeaway from the above results is the behaviour of k with respect to temperature will not cause a grid deformation once LAr equilibrium is reached. With a 5.5 ± 0.2% increase in k from 290K to 87K, the measured values is only 1.3% off from the theoretical prediction of 6.8%, a value which implied a linear dependence of k on E. Thus, both k and the grid strength will increase by approximately the same amount when cooling, causing no deformations to arise with cold.

Additionally, a 5.5% increase in k will correspond to only a 5.5% increase in wire tension (3N to 3.15N), well within the 10N limit for switchback stability.

Pretension and length contraction measurements, while not as precise, do confirm the suspicions that changes in ΔL and T_p are very small. Such changes will have no measurable impact on the stability of the detector.

Detailed error analyses have not been completed on measured values, with the largest contribution to error being estimated and included in plots. This experiment was meant to serve as a general check on the stability of 304 steel springs in cryogenic environments, but data points of utmost precision were certainly not measured.

This experiment focuses only on a small part of the DS-20k wire grid, but results have validated the use of 304 Steel springs as a safety measure. Future experiments will test wire grid planarity, wire bridge friction, E-field holding capacity, etc. culminating in the construction of the final grid by 2025.

Thanks to: Virginia Tech Physics Department, the National Science Foundation, Professor Bruce Vogelaar, Dr. Rijeesh Keloth, Tristan Wright, and Harrison Coombes. This project is funded by No. PHY-2149165

[1] D. Mann, *LNG Materials and Fluids. Ed.* (National Bureau of Standards, Cryogenics Division, 1977).